

# De Novo Formation of Cytokeratin Filament Networks Originates From the Cell Cortex in A-431 Cells

Reinhard Windoffer and Rudolf E. Leube\*

*Department of Anatomy, Johannes Gutenberg-University, Mainz, Germany*

Of the three major cytoskeletal filament systems, the intermediate filaments are the least understood. Since they differ fundamentally from the actin- and microtubule-based networks by their lack of polarity, it has remained a mystery how and where these principally endless filaments are formed. Using a recently established epithelial cell system in which fluorescently labeled intermediate filaments of the cytokeratin type can be monitored in living cells, we address these issues. By multidimensional time-lapse fluorescence microscopy, we examine de novo intermediate filament network formation from non-filamentous material at the end of mitosis and show that it mirrors disassembly. It is demonstrated that filament formation is initiated from the cell cortex without focal preference after cytokinesis. Furthermore, it is shown that this process is dependent on energy, on the integrity of the actin filament network and the microtubule system, and that it can be inhibited by the tyrosine phosphatase inhibitor pervanadate. Based on these observations, a two-step working model is proposed involving (1) interactions within the planar cortical layer acting as an organizing center forming a two-dimensional network and (2) subsequent radial dynamics facilitating the formation of a mature three-dimensional network. *Cell Motil. Cytoskeleton* 50: 33–44, 2001. © 2001 Wiley-Liss, Inc.

**Key words:** cytoskeleton; intermediate filament; mitosis; live cell microscopy; green fluorescent protein

## INTRODUCTION

The in vitro assembly of the 8–12-nm intermediate filaments (IFs) occurs spontaneously and, especially in the case of the epithelial IF polypeptides of the cytokeratin (CK) type, extremely rapidly without any additional factors [Fuchs and Weber, 1994; Herrmann and Aebi, 1998, 2000; Coulombe et al., 2000]. In analogy to the other filament systems, a nucleation event has been proposed to initiate IF elongation, which, however, remains poorly defined [Steinert, 1991b; Herrmann et al., 1996; Abumuhor et al., 1998; Herrmann and Aebi, 1998, 2000; Herrmann et al., 1999; Julien, 1999]. A three-step model has been proposed for in vitro IF formation starting (1) with rapid lateral aggregation of tetramers into “unit-length” filaments, which (2) elongate by longitudinal annealing, and (3) compact from the approximately 20-nm diameter immature filaments into mature 8–12-nm IFs [Herrmann et al., 1996, 1999; Abumuhor et al., 1998; Herrmann and Aebi, 1998, 2000]. The in vivo situation is even less well understood. In interphase cells,

most IF polypeptides are incorporated in IFs, which are in equilibrium with a rather small pool of soluble subunits that are in large part tetrameric although other states of soluble polymers have been detected [Soellner et al., 1985; Chou et al., 1993; Bachant et al., 1996]. The equilibrium is shifted toward the soluble pool during IF breakdown in mitosis [Chou et al., 1993; Omary et al., 1998]. Focal organizing centers have been proposed to act as initiation sites for IF re-formation, among them the nucleus [Eckert et al., 1982; Georgatos and Blobel, 1987; Georgatos et al., 1987; Albers and Fuchs, 1989], certain

Contract grant sponsor: Stiftung Rheinland-Pfalz für Innovation; Contract grant sponsor: German Research Council; Contract grant number: LE 566/7-1.

\*Correspondence to: Rudolf E. Leube, Department of Anatomy, Johannes Gutenberg-University, Becherweg 13, D-55128 Mainz, Germany. E-mail: leube@mail.uni-mainz.de

Received 12 March 2001; Accepted 4 June 2001

cytoplasmic sites [Kreis et al., 1983; Celis et al., 1984; Magin et al., 1990; Raats et al., 1990; Sarria et al., 1990], or plasmamembrane domains [Georgatos et al., 1987; Georgatos and Blobel, 1987] including desmosomes and hemidesmosomes in epithelial cells [Knapp et al., 1983; Bologna et al., 1986]. There is, however, no satisfactory explanation as to how IF formation may be regulated from any of these focal points, as there is common agreement that, due to the absence of defined ends, filament growth is facilitated by lateral exchange of subunits [Vikstrom et al., 1989; Ngai et al., 1990; Miller et al., 1993; Herrmann and Aebi, 1998; Julien, 1999] and not by end-on elongation and shortening as is the case for actin filaments and microtubules.

To examine IF dynamics, we have previously prepared stably transfected, epithelial vulvar carcinoma A-431 clones expressing fluorescent IFs of the CK type [Windoffer and Leube, 1999]. We found that these filaments, which are homogeneously labeled by incorporation of chimerical protein HK13-1 consisting of human CK13 and the enhanced green fluorescent protein EGFP, show an identical distribution and behavior to wild type CK filaments (CKFs). We demonstrate that this cell system (e.g., clone AK13-1) is ideally suited for studying IF assembly and also disassembly because the CKF network disintegrates completely during mitosis, thereby necessitating the de novo formation of two new networks in the daughter cells. With this model system, novel principles of CKF network formation are identified in vivo by 4-D mapping of the CK reorganization in dividing AK13-1 cells. Furthermore, drugs are used to define the contribution of actin filaments, microtubules, energy, and phosphorylation to this process.

## MATERIALS AND METHODS

### Multidimensional Fluorescence Microscopy

Fluorescence microscopy was performed on vulvar carcinoma-derived A-431 subclone AK13-1 stably expressing human CK13-enhanced green fluorescent protein (CK13-EGFP) chimera HK13-1 [Windoffer and Leube, 1999]. For live cell microscopy, logarithmically growing cell cultures were prepared by seeding cells at low density onto 16-mm glass slides one day prior to imaging. The glass slides were then mounted onto a microscope attached culture chamber, and were further maintained in phenol red-free Hanks' medium that was sometimes supplemented with 0.5 mg/ml ascorbic acid [for details see Windoffer and Leube, 1999; Windoffer et al., 2000]. To label chromatin, cells were incubated with vital dye Hoechst 33342 (Molecular Probes, Eugene, OR) at 100 ng/ml in observation medium for 10 min prior to analysis. Fluorescence was recorded with the help of a

confocal laser scanning microscope (Leica TCS NT, Leica Microsystems, Heidelberg, Germany) using an argon laser ( $\lambda = 488$  nm) with dichroic RSP 510, and emission filter BP 530/30. The  $100 \times 1.4$  NA oil PLAPO objective (Leica) was used. Laser power was reduced to prevent phototoxicity while maintaining a sufficient signal to noise ratio. Cells were imaged during different stages of mitosis at time intervals ranging from 0.5 to 2.5 min recording up to ten focal planes from top to bottom with a resolution of either  $1,024 \times 1,024$  pixel or  $512 \times 512$  pixel. Pictures were imported into Photoshop (Adobe) and were arranged into composite figures. Alternatively, images were assembled into movies using ImagePro Plus 4.0 (Media Cybernetics, Silver Spring, CA) and were converted into QuickTime movies (Apple). They are provided at <http://www.uni-mainz.de/FB/Medizin/Anatomie/Leube>.

For highest spatial resolution, cells were fixed with methanol/acetone [see Windoffer and Leube, 1999] and up to 50 focal planes were scanned at  $1,024 \times 1,024$  pixel. Amira (TGS) software was used to prepare animated 3-D reconstructions, which are provided as QuickTime movies on our home page at <http://www.uni-mainz.de/FB/Medizin/Anatomie/Leube>.

For detergent extraction, cells were first fixed for 30 s with a 3% (w/v) formaldehyde solution in PBS, and fluorescence was observed by confocal laser scanning microscopy. During the following treatment with 0.04% (v/v) Triton X-100 (in PBS), changing patterns of CK fluorescence were continuously recorded by time-lapse fluorescence microscopy.

In some instances, drugs were added to AK13-1 cells by replacing the standard medium with medium containing the respective substances. For ATP depletion, sodium azide (0.05% [w/v]; Sigma, St. Louis, MO) and deoxyglucose (50 mM final concentration; Sigma) were added to the recording medium [see Yoon et al., 1998]. For disruption of actin filaments, cytochalasin D (2  $\mu$ M final concentration; Sigma) [see Windoffer and Leube, 1999] was used; for disruption of microtubules, nocodazole (1  $\mu$ M final concentration; Sigma) was used [see Windoffer and Leube, 1999]. To inhibit tyrosine phosphatases,  $\text{Na}_3\text{VO}_4$  (20 mM final concentration; Sigma) was added to standard medium, and was activated by treatment with 16.3 mM  $\text{H}_2\text{O}_2$  and 200  $\mu$ g/ml catalase (Sigma) 5 min prior to application to the cells [Imbert et al., 1994].

### Quantification of Gray Values

Measurement areas corresponding to the cytoplasm of single mitotic cells were selected manually. Using ImagePro Plus, gray values were determined for each pixel within this area. With Excel (Microsoft) the sum of all gray values less than 255 was calculated for each time

point. White pixels (gray value of 255) were excluded assuming that they correspond to aggregated and/or filamentous CKs. The mean gray value was determined and used for graphical representation of time-dependent changes.

## RESULTS

### Complete Cytokeratin Filament Network Disassembly into Soluble and Granular Material in AK13-1 Cells During Mitosis

Confocal laser scanning microscopy was performed on AK13-1 cells stably expressing human CK13-EGFP chimera HK13-1 to determine the complete spatial distribution of all CK material in single cells during interphase and mitosis. Figure 1A and the corresponding movie 1 show the typical fluorescence pattern of HK13-1 in an interphase cell. A dense band of filament bundles encircles the nucleus from which filaments extend forming a network that envelops the entire nucleus and projects toward the cell periphery where desmosomal contact sites are located. In the free cell margin, diffuse material and thin filament-like structures were seen, which we have previously shown to move continuously inward in an ATP- and microtubule-dependent manner [Windoffer and Leube, 1999]. A very different situation was encountered during metaphase (Fig. 1B; animation in movie 2) when, instead, local concentrations of non-filamentous material were visualized in the form of variably sized spheroid granules and rodlets that were usually concentrated in the cell periphery, and when a strong diffuse labeling was detected throughout the cytoplasm. This showed that the CKF network was completely broken down into non-filamentous assemblies at this time point during mitosis and excludes that, in contrast to earlier studies in which only single focal planes were recorded [Windoffer and Leube, 1999], residual filaments remained in specific subcellular regions that could act as initiation sites for network re-formation.

To further define the different types of CK fluorescence, AK13-1 cells were subjected to treatment with the non-ionic detergent Triton X-100 at low concentration. While this treatment did not significantly affect the fluorescence in interphase cells (not shown), it removed all of the diffuse cytoplasmic and some of the cortical fluorescence from mitotic cells (Fig. 2) indicating the presence of a considerable amount of soluble CKF subunits that were extracted by the detergent. The remaining granular Triton X-100-resistant material in mitotic cells corresponds to the non-filamentous CK aggregates that have been known for a long time and have been characterized in detail [e.g., Franke et al., 1982; Lane et al., 1982; Jones et al., 1985].

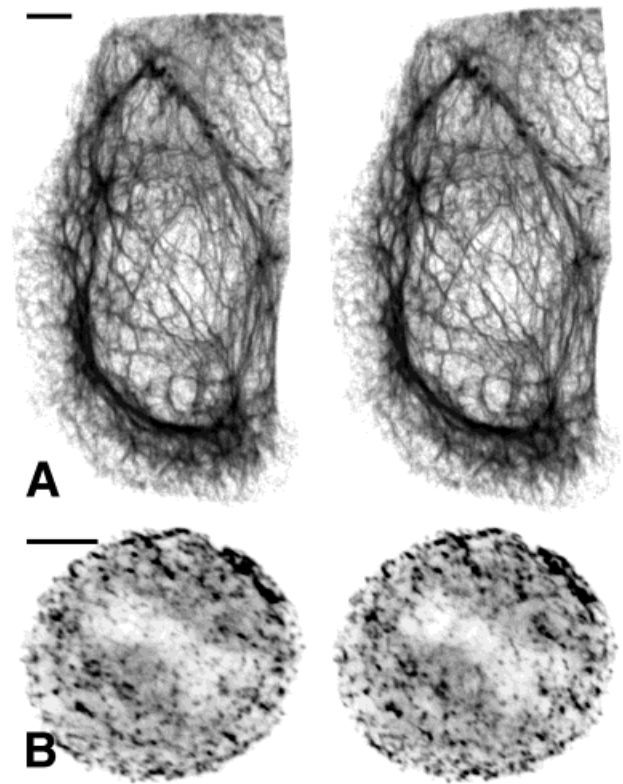


Fig. 1. Stereo pairs of superimposed serial sections (46 in A, 25 in B) depicting inverse fluorescence images of human CK13-EGFP chimera HK13-1 in stably transfected AK13-1 cells during interphase (A) and metaphase (B). Stacks of fluorescence images were also converted into animated 3-D reconstructions (movies 1 and 2 at <http://www.uni-mainz.de/FB/Medizin/Anatomie/Leube>). Note the typical CKF organization in A and movie 1 with thick perinuclear cables extending toward the cell periphery to desmosomal contact sites and the relative scarcity of filament bundles in cortical domains of the free cell edge. In contrast, no filaments are seen in B and movie 2 where instead considerable, diffuse fluorescence is detectable throughout the cytoplasm, and where aggregated material in the form of variably shaped granules and short rods is present predominantly in the cortical region. Scale bars = 5  $\mu$ m.

### Stages of Cytokeratin Filament Network Formation

3-D time-lapse fluorescence microscopy of dividing AK13-1 cells was performed to find out where and how CKF network formation is accomplished starting from the pools of soluble and aggregated material in mitotic cells. The time point 0 min in Figure 3A depicts the fluorescence recorded in four focal planes of a mitotic AK13-1 cell with a forming cleavage furrow at the onset of cytokinesis. The fluorescence distribution is similar to that shown in Figure 1B with diffuse cytoplasmic staining and multiple granules and rodlets most of which are located in the cortical region. Subsequent fluorescence images are provided as movie 3 and representative stages taken from there are depicted in Figure 3. At 2.5 min,

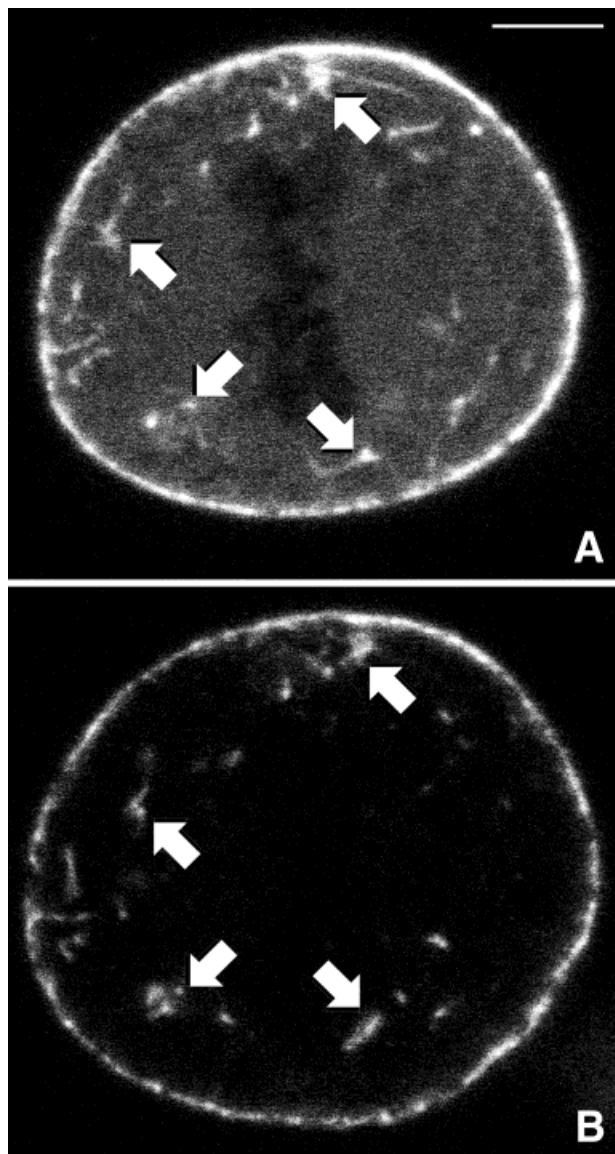


Fig. 2. Fluorescence microscopy of a formaldehyde-fixed AK13-1 cell during metaphase detecting human CK13-EGFP chimera HK13-1 before (A) and after a 10-min treatment with 0.04% Triton X-100 (B) using identical recording parameters. Note the complete loss of diffuse cytoplasmic fluorescence after detergent extraction and the retention of granular material in the cytoplasm (arrows) and cortical region. The ballooning of the cell is probably due to osmosis-induced fluid influx. Scale bar = 5  $\mu$ m.

some of the rodlets had fused forming branched structures. This process was clearly visible in the central cytoplasm (level 2 at 2.5 min in Fig. 3A) but was most pronounced in the cell cortex where a coarse and incomplete network appeared (see level 1 at 2.5 min in Fig. 3A and 7.5 min in Fig. 3C). Later on, practically all granules and rodlets disappeared in the central cytoplasm whereas cortical fluorescence intensity increased further (compare level 2 at 2.5 and 22.5 min in Fig. 3A). Movies taken at

higher frequency showed that some cytoplasmic granules and rodlets fused with the cortical material (not shown). In contrast to the unsuccessful cytoplasmic network formation, cortical branched structures continued to build up a network with increasingly finer mesh size and progressively thinner-appearing filaments (compare level 1 at 22.5 and 62.5 min in Fig. 3A, or 7.5 min with 12.5 min in Fig. 3C). A cortical CKF network was already discernible at a time when no network was seen in the central cytoplasm (compare 12.5 min in Fig. 3C with level 2 at 22.5 min in Fig. 3A). The fine cortical network started to spread only later toward the central cytoplasm in a continuous centripetal movement (compare 22.5, 62.5, and 112.5 min of level 2 in Fig. 3A). A gradual reduction of diffuse cytoplasmic fluorescence was noted concurrent to network formation and extension. Quantification of gray values confirmed this impression (Fig. 4A). Taken together, we conclude that *de novo* CKF network formation originates without focal preference from the entire cell cortex where diffuse and aggregated material initiates the formation of a progressively finer network that subsequently extends toward the central cytoplasm.

#### Stages of Cytokeratin Filament Disassembly

To better understand mechanisms of mitotic CKF reorganization, we also examined CKF network disassembly. In order to study this process, it was necessary to identify early stages of mitosis in living AK13-1 cells. To this end, chromatin was labeled with vital dye Hoechst 33342. At the start of chromatin condensation determined in this way, CKF disassembly was already in progress while the nuclear envelope was still intact and rounding of cells was barely noticeable. Zero minutes in Figure 5 shows such a situation taken from a 3-D time-lapse recording (movie 4). Note that, in contrast to interphase (Fig. 1A), the filament network was restricted to the peripheral cytoplasm whereas the central cytoplasmic region was devoid of filaments, containing instead small pleomorphic fragments and diffuse fluorescence. At subsequent stages (Fig. 5, movie 4), the filamentous fluorescence retracted progressively toward the cell periphery. At the same time, the diffuse fluorescence increased further, and rod-like or branched fragments appeared in the cytoplasm that either changed shape forming spheroid granules or disappeared. The cortical network became increasingly coarse being composed of thicker-appearing filaments with interspersed granular enrichments (32.5 min in Fig. 5C). Finally, the remaining cortical network disintegrated rapidly into small granules (within less than 7.5 min; compare 32.5 min and 40 min in Fig. 5C). At the end of the sequence, most of the spheroid granular aggregates were located in the cell periphery where they appeared to be anchored to the cell cortex in

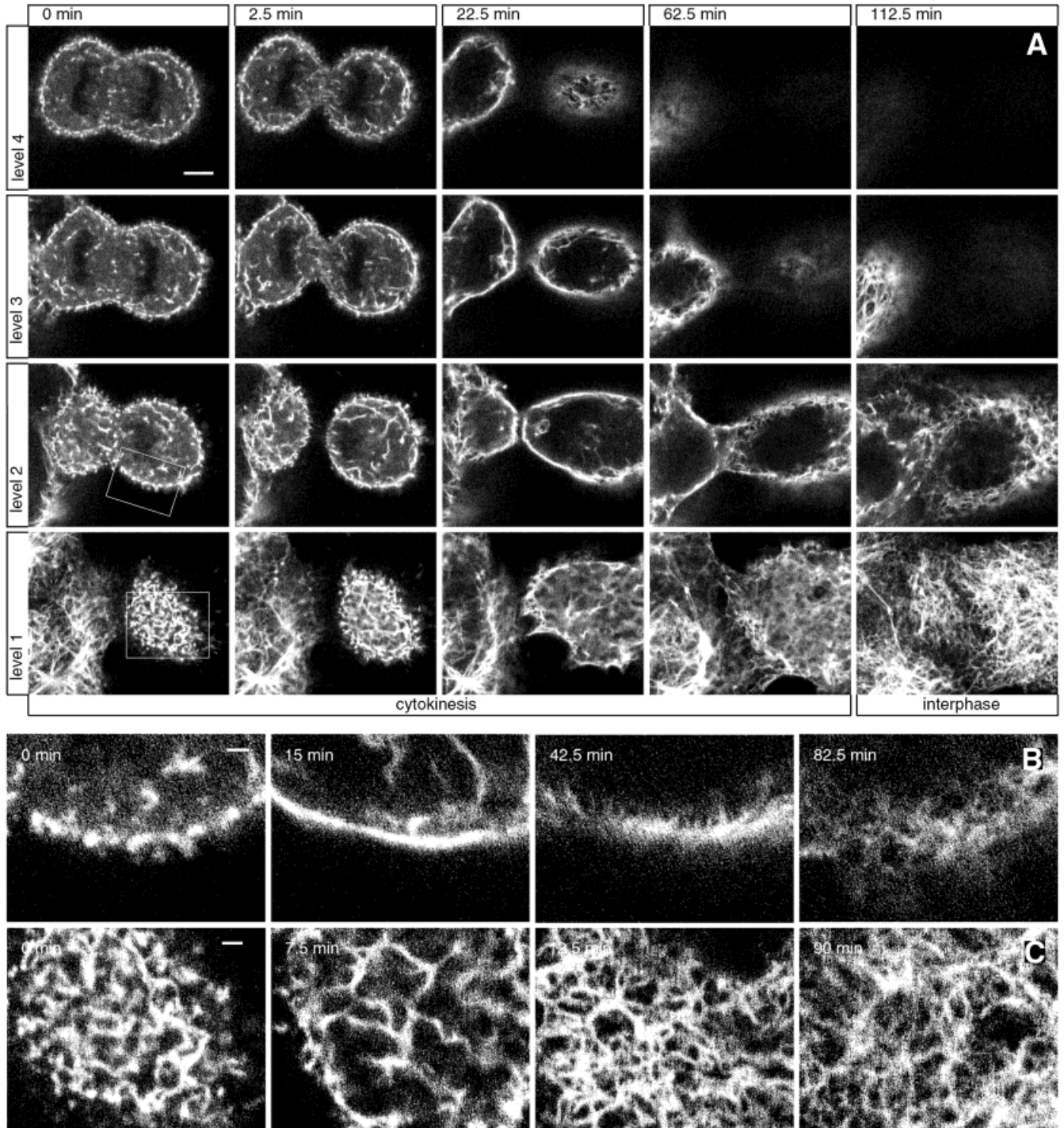


Fig. 3. Fluorescence microscopy showing stages of CKF formation at the end of mitosis in A-431 clone AK13-1 stably expressing human CK13-EGFP chimera HK13-1. The micrographs are taken from a recording of four different focal planes (levels 1–4) that are provided as movie 3 at <http://www.uni-mainz.de/FB/Medizin/Anatomie/Leube>. **A**: At time point 0 min, the cell has entered cytokinesis and formation of the cleavage furrow is in progress. Granules and rodlets are seen in the cytoplasm and are enriched in the cell cortex at that time. Some

cytoplasmic rodlets further elongate (2.5 min) but disappear later (22.5 min). Rebuilding of a typical CKF network originates from the cell periphery and proceeds toward the cell center. Note that diffuse cytoplasmic fluorescence decreases during filament formation. Simultaneously, cells flatten and re-establish extensive contacts with neighboring cells. Scale bar = 5  $\mu\text{m}$ . **B,C**: Enlargements of cell cortex corresponding to areas demarcated by boxes in A showing either transverse (B) or en face view (C). Scale bars = 2  $\mu\text{m}$ .

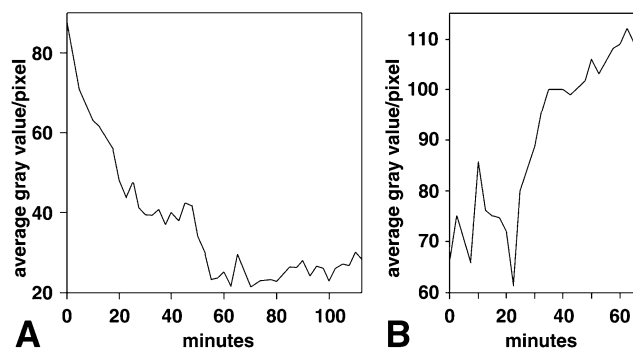


Fig. 4. Diagram depicting kinetics of diffuse HK13-1 fluorescence in AK13-1 cells during CKF assembly (A) and disassembly (B). Fluorescence was quantified inside dividing cells by measurements of gray values. Values in A were taken from level 2 of movie 3 (compare Fig. 3); values in B from level 2 of movie 4 (compare Fig. 5). The complete movies are provided at <http://www.uni-mainz.de/FB/Medizin/Anatomie/Leube>. The decrease of gray value per pixel during filament formation and the increase of gray value per pixel during filament breakdown are due to reversible CKF subunit polymerization and solubilization, respectively.

contrast to the highly mobile but morphologically indistinguishable granules in the cytoplasm. Typically, this CK fluorescence pattern remained the same until the cleavage furrow began to form (see Fig. 3). The steadily increasing diffuse fluorescence during prometaphase was also quantified by determination of gray values showing that it paralleled the progressing CKF disassembly (Fig. 4B). In conclusion, CKF breakdown appears to involve mechanisms with features reminiscent of filament formation but occurring in the reverse order.

#### Importance of Energy, Actin Filaments, Microtubules, and Phosphorylation for Cytokeratin Filament Network Formation

In the next set of experiments, we wanted to identify factors that contribute to CKF network formation in mitotic cells. Based on our previous observations in which we demonstrated energy-dependent CKF dynamics in AK13-1 cells during interphase [Windoffer and Leube, 1999], we treated dividing cells with deoxyglucose and sodium azide to deplete ATP reservoirs. The drugs were added during late cytokinesis when cleavage was almost complete, i.e., at a time point just prior to the onset of CKF formation. Within less than 10 min after addition of the drugs, CK dynamics stopped and the overall distribution pattern remained the same for the rest of the observation period (Fig. 6; compare control movie 5 with movie 6). Hardly any mobility of fluorescent structures was seen similar to the situation observed in ATP-depleted interphase cells [Windoffer and Leube, 1999]. Removal of the substances resulted in subsequent normal CKF network formation (not shown).

To elucidate the importance of the actin filament system for CKF network formation, cells were treated with cytochalasin D previously shown to be necessary for the maintenance of an extended CKF system in AK13-1 cells during interphase [Windoffer and Leube, 1999]. The drug was added after cells had separated. Twenty minutes after addition, cortical material moved toward the cell center (movie 7). But, in contrast to untreated cells, the material remained coarse and did not form a fine filamentous network extending throughout the cell (compare control and cytochalasin D-treated cells in Fig. 6, and movie 5 with movie 7). Next, cells were treated with the microtubule-disrupting agent nocodazole, which interferes with inward-directed CK motility in interphase AK13-1 cells [Windoffer and Leube, 1999]. In this instance, fluorescent material was almost completely recruited into the cortical region where it was retained during the rest of the observation period extending only minimally toward the cell center (Fig. 6; movie 8). Its organization changed, however, from highly concentrated to more diffuse (compare, e.g., 30 and 90 min in nocodazole-treated cells of Fig. 6).

To examine the contribution of phosphorylation for CKF network formation, AK13-1 cells were treated with pervanadate, a reagent known to inhibit phosphatases, thereby increasing tyrosine phosphorylation, and to affect CKF organization in interphase cells [Feng et al., 1999] including also AK13-1 cells where we observed a rapid CKF breakdown in interphase (not shown). Application of this drug efficiently prevented CKF network formation at the end of mitosis. Instead, fluorescent, non-filamentous material remained in the cortical region (Fig. 6; movie 9).

#### DISCUSSION

In contrast to the rapid and spontaneous formation of CKFs *in vitro* [Herrmann and Aebi, 1998, 2000], CKF formation is prevented in our cell system during mitosis despite the presence of abundant CK polypeptides that are kept in a soluble or aggregated non-filamentous state most likely due to protein modification, i.e., phosphorylation [Omary et al., 1998]. Our system of vimentin-free dividing AK13-1 cells, in which the cytoplasmic IF network is completely disassembled, differs from previous experimental setups in which either the same or other cytoplasmic IFs were present and could potentially aid in filament formation [Kreis et al., 1983; Franke et al., 1984; Vikstrom et al., 1989; Magin et al., 1990; Ngai et al., 1990; Raats et al., 1990; Sarria et al., 1990; Bader et al., 1991; Miller et al., 1993]. By monitoring CK chimera HK13-1 in dividing cells, we show that filament assembly and disassembly are temporospatially regulated and

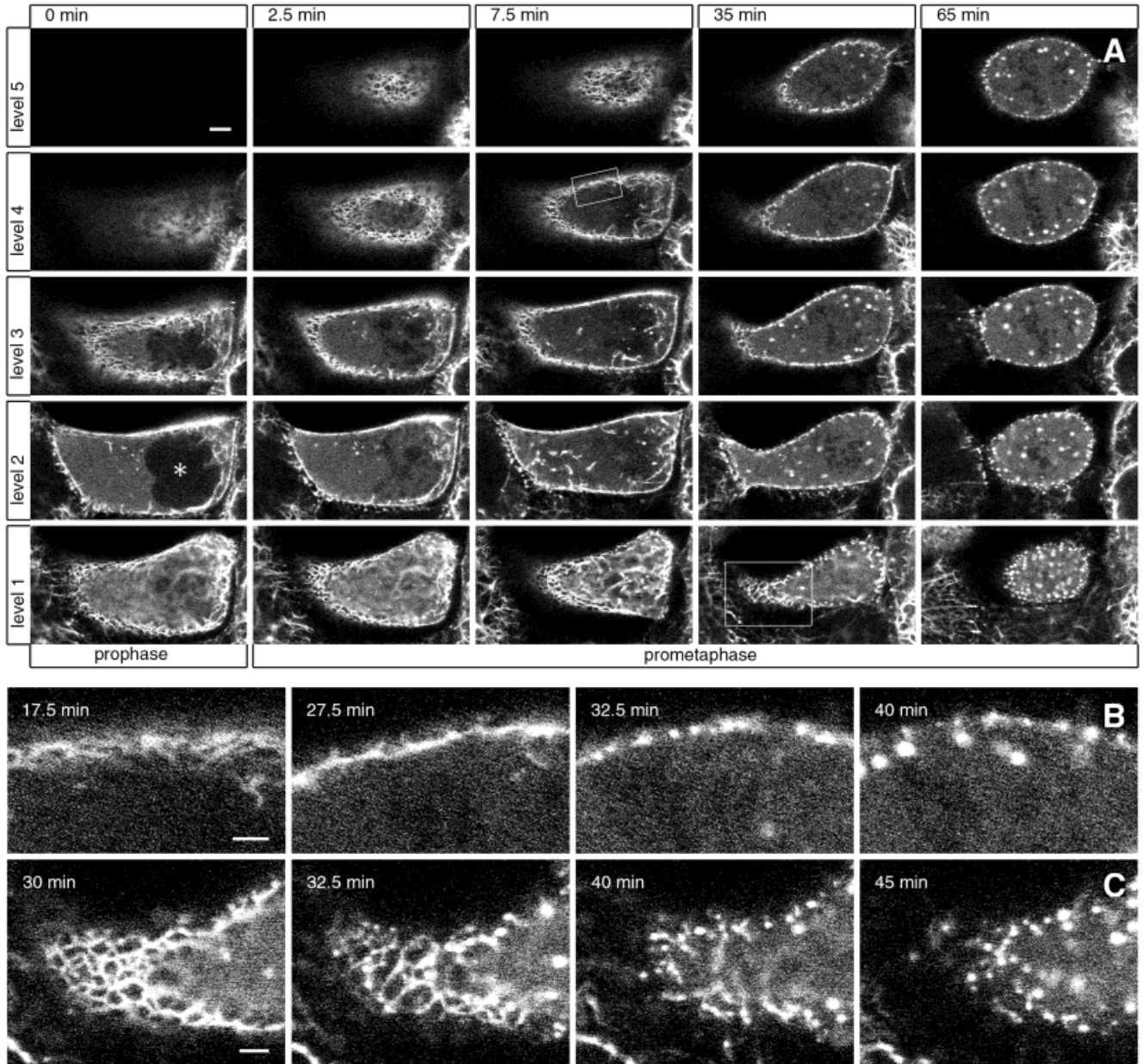


Fig. 5. Selected fluorescence micrographs taken from a time-lapse recording depicting the complete breakdown of the CKF network in a dividing cell from early prophase to late prometaphase. Using confocal scanning laser microscopy, images were obtained from human vulvar carcinoma-derived A-431 subclone AK13-1 stably expressing fluorescent CKFs containing human CK13-EGFP chimera HK13-1. The entire recording is provided as movie 4 (<http://www.uni-mainz.de/FB/Medizin/Anatomie/Leube>). **A:** Five focal planes from bottom to top (levels 1–5) at five time points. At the beginning of the recording (early prophase), partial filament breakdown has already taken place in central cytoplasmic regions and increased diffuse cytoplasmic staining

can be seen. At that point, the nucleus (\*) is still intact. Filament disassembly continues from the center of the cell towards the periphery, where the originally fine network concentrates in more solid structures and disintegrates into granules. Note, that at the end of the sequence CKFs are completely absent. Instead, significant diffuse cytoplasmic staining and granules, most of which are located in the cell periphery, are detected in the rounded cells. At some intermediate time points rodlets arise in the cytoplasm (e.g., level 2, 7.5 min) but disappear later. Scale bar = 5 μm. **B,C:** High magnifications of cortical regions are taken from outlined areas in a showing either transverse (B) or en face view (C). Scale bars = 2 μm.

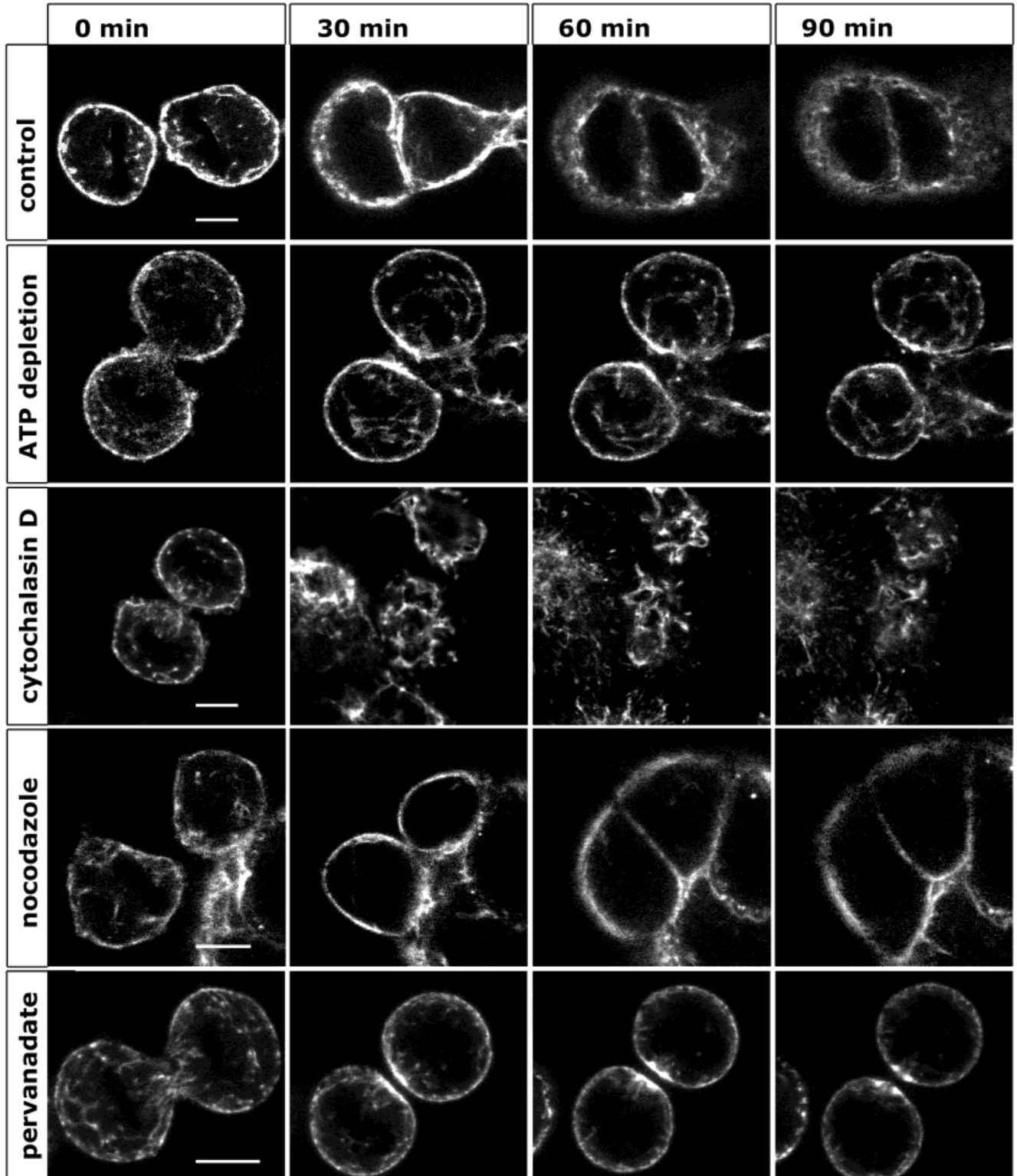


Fig. 6. Time-lapse fluorescence microscopy of dividing AK13-1 cells depicting the distribution of human CK13-EGFP chimera HK13-1 in the presence of different drugs (**top**, untreated control cells). Each panel shows four time points each taken from stacks of confocal images that were recorded at 90-s intervals. The complete time series of pictures are provided as movies 5–9 at <http://www.uni-mainz.de/FB/Medizin/Anatomie/Leube>. For ATP depletion, cells were

treated with 0.05% [w/v] sodium azide and 50 mM deoxyglucose. Actin filament organization was disrupted by cytochalasin D (2  $\mu$ M), microtubules by nocodazole (1  $\mu$ M). **Bottom**: HK13-1 in dividing cells treated with the tyrosine phosphatase inhibitor pervanadate (20 mM). Note the specific differences occurring in each case of drug treatment in comparison to control cells. Scale bars = 5  $\mu$ m.

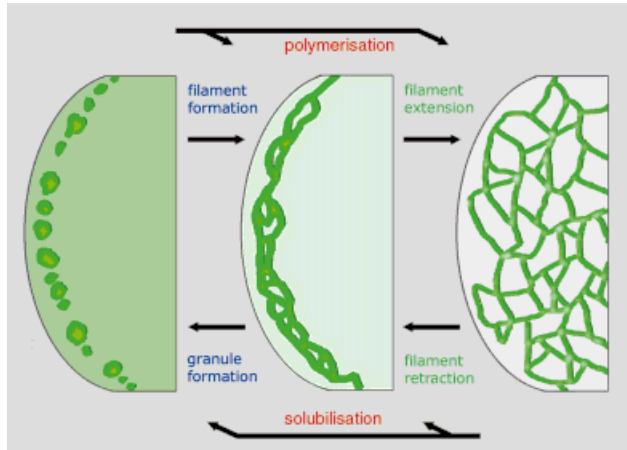


Fig. 7. Simplified two-step model highlighting major aspects of CKF network assembly (from left to right) and disassembly (from right to left) occurring during mitosis. For simplicity's sake, granules and rodlets occurring in the central cytoplasm are not depicted, since they do not directly contribute to network formation. **Left:** Step involves alternate decisions regarding granule extension and rodlet ligation vs. filament fragmentation and granular aggregate formation. **Right:** Step is characterized by radial filament extension and thinning of filaments during network formation, and, conversely, by CKF retraction toward the cell cortex and filament thickening during network disassembly. Gradients of increasing filament polymerization or increasing filament solubilization occur throughout assembly and disassembly, respectively. For further details concerning the nature of the reversible mechanisms, see text.

reversible. Based on our observations we can distinguish three different contributing processes (see scheme in Fig. 7):

1. Polymerization and solubilization of filaments by exchange with a soluble subunit pool. This process presents itself in our movies as continuously decreasing or increasing cytoplasmic fluorescence during filament assembly and disassembly, respectively (Fig. 4). It is most likely determined by protein modification, since the increased CK phosphorylation occurring during mitosis correlates well with the elevated soluble CK pool [Inagaki et al., 1996; Omary et al., 1998]. Accordingly, we could prevent CKF reformation by treatment of AK13-1 cells with the tyrosine phosphatase inhibitor pervanadate that, due to its rapid action (own unpublished results), may directly affect the phosphorylation of HK13-1 [for other CKs see Feng et al., 1999]. Exchange of soluble subunits does not occur at specialized filament ends but takes place uniformly throughout existing filaments by lateral addition and removal [Franke et al., 1984; Vikstrom et al., 1989; Ngai et al., 1990; Miller et al., 1993; Herrmann and Aebi, 1998; Julien, 1999]. The detection of progressively thinner-

appearing filamentous material during network formation and the observation of a rather coarse filamentous net with thick filament bundles during network breakdown in our movies support the importance of lateral growth dynamics for the CKF system during mitosis.

2. Filament formation by granule elongation and ligation, and filament disassembly by fragmentation and aggregation. During CKF assembly we observed elongation of spheroid aggregates into rodlets that subsequently fused into longer rods and branched networks. Conversely, during CKF disassembly rod-like fragments appeared that seemed to condense into spheroid aggregates. Evidence has been obtained in other systems for the existence of oligomeric CKF fragments both during assembly and disassembly [Klymkowsky et al., 1991; Steinert, 1991a; Bachant and Klymkowsky, 1996; Gard and Klymkowsky, 1998]. The molecular details of the observed CKF ligating or cleaving activities occurring during mitosis are not known. Although specific enzyme-mediated cleavage by caspases has been shown to be responsible for CK fragmentation in apoptotic cells [Caulin et al., 1997; Ku and Omary, 1997], cleaving and ligating activities cannot be due to creating or breaking covalent bonds during mitosis but rather involve non-covalent, such as hydrophobic or charge, interactions to facilitate the rapid switching between the non-filamentous and filamentous CK state that does not require protein synthesis. It should be stressed that the fragments seen in our cells are comparatively rare, indicating that either ligation and fragmentation are minor mechanisms and/or that both reactions occur rapidly. It is also remarkable that, although rodlets are formed from spheroid granules in all cytoplasmic domains, only those in the cortex but not those in the central cytoplasm are capable of forming a CKF network as might have been expected from earlier ectopic expression studies [Kreis et al., 1983; Franke et al., 1984; Magin et al., 1990; Bader et al., 1991]. It is, therefore, concluded that specific factors determine whether a filament network can be formed or not. These factors must be under specific temporal and spatial control, since aggregate formation is restricted to mitosis and filament network re-formation is only successful in the cell cortex but not in the cytoplasm at the end of mitosis.
3. Extension and retraction of CKF nets from and to the cell cortex. This process, which we de-

scribe for the first time in mitotic cells, is visualized in our movies as the spreading of CKFs from the cortex during network formation and retraction of the network during disintegration. In this context, it is interesting that an increasing number of publications provides evidence for such a mechanism in interphase, which is based on the linkage of the IF system to the other major filament-networks, thereby not only determining cortical localization of IFs [Gard et al., 1997; Gard and Klymkowsky, 1998; Windoffer and Leube, 1999] but also facilitating radial IF motility [Tint et al., 1991; Ho et al., 1998; Prahlad et al., 1998, 2000; Yoon et al., 1998; Martys et al., 1999; Windoffer and Leube, 1999; Chou and Goldman, 2000; Shah et al., 2000; Chou et al., 2001]. Furthermore, we already presented results in our system indicating that the cell cortex may function as a source for CKF replenishment during interphase by continuously providing filaments and filament precursors that are continuously transported into the more central IF cytoskeleton in an energy- and microtubule-dependent fashion [Windoffer and Leube, 1999]. Termination of this movement at the beginning of mitosis would, therefore, result in apparent network retraction whereas re-activation of this motility would induce extension of a new network. In support of this, energy depletion and microtubule disruption during cytokinesis prevented network extension from the cell periphery. Also, the cytochalasin D-induced collapse of cortical CK material and the incomplete network formation further underscore this notion.

Our finding that filament network dynamics are controlled from the cell cortex by affecting successful ligation of rodlets into networks and by determining CKF extension vs. retraction, identifies the cell cortex as an organizing center where, depending on the mitotic stage, differential decisions are made. This contrasts with previous studies that implicated the nucleus and cytoplasmic foci, or specialized membrane sites acting as initiation sites for IF network formation [Eckert et al., 1982; Knapp et al., 1983; Kreis et al., 1983; Celis et al., 1984; Bologna et al., 1986; Georgatos and Blobel, 1987; Georgatos et al., 1987; Albers and Fuchs, 1989; Magin et al., 1990; Raats et al., 1990; Sarria et al., 1990; Djabali, 1999]. By immunoelectronmicroscopy, we found strong labeling of a circumferential layer of non-filamentous material just below the actin cortical mesh after complete filament breakdown (not shown). Earlier studies have also reported the presence of cortically-restricted granules in

the same location of mitotic epithelial cells [Lane et al., 1982].

## CONCLUSIONS

Based on our findings, a two-step model is proposed (Fig. 7). It accounts for both CKF assembly and disassembly as reverse processes that are driven by the same basic machinery employing the identified mechanisms. Continuously changing equilibria between filament polymerization and solubilization accompany both steps of filament network formation and disruption, and reach steady state only during interphase. The step depicted in Figure 7 (left) is characterized by interactions within the planar and borderless cortical layer. Thus, an endless filament network may be formed by non-directional interactions of subunits due to local mechanisms favoring rodlet formation over granule formation and ligation over fragmentation. The model also implies that the initiation of filament formation takes place within this layer by association of assembly-competent subunits. These ideas are compatible with *in vitro* observations demonstrating the formation of “unit-length” lateral aggregates of tetramers, their annealing into “immature,” large diameter filaments and compaction into mature 11-nm filaments [Herrmann et al., 1996, 1999; Herrmann and Aebi, 1998]. The other step depicted in Figure 7 (right) is characterized by radial filament movement along axes all of which are perpendicular to the cortex. It relies on active transport mechanisms facilitated by the other polar filament systems. This part of the model explains how the transition between the planar, transitory, and cortex-restricted mitotic network and the three-dimensional cytoplasmic interphase network is accomplished. Thereby, vectorial organizational principles are imposed on the intrinsically apolar IFs without disrupting their continuity. With the proposed model that is derived from *in vivo* observations, working hypotheses are provided that will help to further elucidate the peculiar molecular mechanisms that determine the formation of CKFs. Given the structural and functional complexity of IF proteins the challenge will be to find out if and to what extent the proposed model or certain modifications thereof apply to other cell types and other IFs.

## ACKNOWLEDGMENTS

We thank Ursula Wilhelm and Bernhard Beile for expert technical assistance.

## REFERENCES

- Abumuhor IA, Spencer PH, Cohlberg JA. 1998. The pathway of assembly of intermediate filaments from recombinant alpha-internexin. *J Struct Biol* 123:187–198.
- Albers K, Fuchs E. 1989. Expression of mutant keratin cDNAs in epithelial cells reveals possible mechanisms for initiation and assembly of intermediate filaments. *J Cell Biol* 108:1477–1493.
- Bachant JB, Klymkowsky MW. 1996. A nontetrameric species is the major soluble form of keratin in *Xenopus* oocytes and rabbit reticulocyte lysates. *J Cell Biol* 132:153–165.
- Bader BL, Magin TM, Freudenmann M, Stumpp S, Franke WW. 1991. Intermediate filaments formed de novo from tail-less cytokeratins in the cytoplasm and in the nucleus. *J Cell Biol* 115:1293–1307.
- Bologna M, Allen R, Dulbecco R. 1986. Organization of cytokeratin bundles by desmosomes in rat mammary cells. *J Cell Biol* 102:560–567.
- Caulin C, Salvesen GS, Oshima RG. 1997. Caspase cleavage of keratin 18 and reorganization of intermediate filaments during epithelial cell apoptosis. *J Cell Biol* 138:1379–1394.
- Celis JE, Small JV, Larsen PM, Fey SJ, De Mey J, Celis A. 1984. Intermediate filaments in monkey kidney TC7 cells: focal centers and interrelationship with other cytoskeletal systems. *Proc Natl Acad Sci USA* 81:1117–1121.
- Chou CF, Riopel CL, Rott LS, Omary MB. 1993. A significant soluble keratin fraction in 'simple' epithelial cells. Lack of an apparent phosphorylation and glycosylation role in keratin solubility. *J Cell Sci* 105:433–444.
- Chou YH, Goldman RD. 2000. Intermediate filaments on the move. *J Cell Biol* 150:F101–106.
- Chou Y-H, Helfand BT, Goldman RD. 2001. New horizons in cytoskeletal dynamics: transport of intermediate filaments along microtubule tracks. *Curr Opin Cell Biol* 13:106–109.
- Coulombe PA, Bousquet O, Ma L, Yamada S, Wirtz D. 2000. The 'ins' and 'outs' of intermediate filament organization. *Trends Cell Biol* 10:420–428.
- Djabali K. 1999. Cytoskeletal proteins connecting intermediate filaments to cytoplasmic and nuclear periphery. *Histol Histopathol* 14:501–509.
- Eckert BS, Daley RA, Parysek LM. 1982. Assembly of keratin onto PtK1 cytoskeletons: evidence for an intermediate filament organizing center. *J Cell Biol* 92:575–578.
- Feng L, Zhou X, Liao J, Omary MB. 1999. Pervanadate-mediated tyrosine phosphorylation of keratins 8 and 19 via a p38 mitogen-activated protein kinase-dependent pathway. *J Cell Sci* 112:2081–2090.
- Franke WW, Schmid E, Grund C, Geiger B. 1982. Intermediate filament proteins in nonfilamentous structures: transient disintegration and inclusion of subunit proteins in granular aggregates. *Cell* 30:103–113.
- Franke WW, Schmid E, Mittnacht S, Grund C, Jorcano JL. 1984. Integration of different keratins into the same filament system after microinjection of mRNA for epidermal keratins into kidney epithelial cells. *Cell* 36:813–825.
- Fuchs E, Weber K. 1994. Intermediate filaments: structure, dynamics, function, and disease. *Annu Rev Biochem* 63:345–382.
- Gard DL, Klymkowsky MW. 1998. Intermediate filament organization during oogenesis and early development in the clawed frog, *Xenopus laevis*. In: Herrmann H, Harris JR, editors. *Subcellular biochemistry: intermediate filaments*. Vol 31. New York: Plenum Press. p 35–70.
- Gard DL, Cha BJ, King E. 1997. The organization and animal-vegetal asymmetry of cytokeratin filaments in stage VI *Xenopus* oocytes is dependent upon F-actin and microtubules. *Dev Biol* 184:95–114.
- Georgatos SD, Blobel G. 1987. Two distinct attachment sites for vimentin along the plasma membrane and the nuclear envelope in avian erythrocytes: a basis for a vectorial assembly of intermediate filaments. *J Cell Biol* 105:105–115.
- Georgatos SD, Weber K, Geisler N, Blobel G. 1987. Binding of two desmin derivatives to the plasma membrane and the nuclear envelope of avian erythrocytes: evidence for a conserved site-specificity in intermediate filament-membrane interactions. *Proc Natl Acad Sci USA* 84:6780–6784.
- Herrmann H, Aebi U. 1998. Structure, assembly, and dynamics of intermediate filaments. In: Herrmann H, Harris JR, editors. *Subcellular biochemistry: intermediate filaments*. Vol 31. New York: Plenum Press. p 319–362.
- Herrmann H, Aebi U. 2000. Intermediate filaments and their associates: multi-talented structural elements specifying cytoarchitecture and cytodynamics. *Curr Opin Cell Biol* 12:79–90.
- Herrmann H, Haner M, Brettel M, Müller SA, Goldie KN, Fedtke B, Lustig A, Franke W, Aebi U. 1996. Structure and assembly properties of the intermediate filament protein vimentin: the role of its head, rod and tail domains. *J Mol Biol* 264:933–953.
- Herrmann H, Haner M, Brettel M, Ku NO, Aebi U. 1999. Characterization of distinct early assembly units of different intermediate filament proteins. *J Mol Biol* 286: 1403–1420.
- Ho CL, Martys JL, Mikhailov A, Gundersen GG, Liem RK. 1998. Novel features of intermediate filament dynamics revealed by green fluorescent protein chimeras. *J Cell Sci* 111:1767–1778.
- Imbert V, Peyron JF, Farahi Far D, Mari B, Auberger P, Rossi B. 1994. Induction of tyrosine phosphorylation and T-cell activation by vanadate peroxide, an inhibitor of protein tyrosine phosphatases. *Biochem J* 297:163–173.
- Inagaki I, Matsuoka Y, Tsujimura K, Ando S, Tokui T, Takahashi T, Inagaki N. 1996. Dynamic property of intermediate filaments: regulation by phosphorylation. *BioEssays* 18:481–487.
- Jones JC, Goldman AE, Yang HY, Goldman RD. 1985. The organizational fate of intermediate filament networks in two epithelial cell types during mitosis. *J Cell Biol* 100:93–102.
- Julien JP. 1999. Neurofilament functions in health and disease. *Curr Opin Neurobiol* 9:554–560.
- Klymkowsky MW, Maynell LA, Nislow C. 1991. Cytokeratin phosphorylation, cytokeratin filament severing and the solubilization of the maternal mRNA Vg1. *J Cell Biol* 114:787–797.
- Knapp LW, O'Guin WM, Sawyer RH. 1983. Rearrangement of the keratin cytoskeleton after combined treatment with microtubule and microfilament inhibitors. *J Cell Biol* 97:1788–1794.
- Kreis TE, Geiger B, Schmid E, Jorcano JL, Franke WW. 1983. De novo synthesis and specific assembly of keratin filaments in nonepithelial cells after microinjection of mRNA for epidermal keratin. *Cell* 32:1125–1137.
- Ku NO, Omary MB. 1997. Phosphorylation of human keratin 8 in vivo at conserved head domain serine 23 and at epidermal growth factor-stimulated tail domain serine 431. *J Biol Chem* 272: 7556–7564.
- Lane EB, Goodman SL, Trejdosiewicz LK. 1982. Disruption of the keratin filament network during epithelial cell division. *EMBO J* 1:1365–1372.
- Magin TM, Bader BL, Freudenmann M, Franke WW. 1990. De novo formation of cytokeratin filaments in calf lens cells and cytoplasts after transfection with cDNAs or microinjection with mRNAs encoding human cytokeratins. *Eur J Cell Biol* 53:333–348.
- Martys JL, Ho CL, Liem RK, Gundersen GG. 1999. Intermediate filaments in motion: observations of intermediate filaments in

- cells using green fluorescent protein-vimentin. *Mol Biol Cell* 10:1289–1295.
- Miller RK, Khuon S, Goldman RD. 1993. Dynamics of keratin assembly: exogenous type I keratin rapidly associates with type II keratin in vivo. *J Cell Biol* 122:123–135.
- Ngai J, Coleman TR, Lazarides E. 1990. Localization of newly synthesized vimentin subunits reveals a novel mechanism of intermediate filament assembly. *Cell* 60:415–427.
- Omary MB, Ku NO, Liao J, Price D. 1998. Keratin modifications and solubility properties in epithelial cells and in vitro. In: Herrmann H, Harris JR, editors. *Subcellular biochemistry: intermediate filaments*. Vol 31. (ed.) New York: Plenum Press. p 105–140.
- Prahlad V, Yoon M, Moir RD, Vale RD, Goldman RD. 1998. Rapid movements of vimentin on microtubule tracks: kinesin-dependent assembly of intermediate filament networks. *J Cell Biol* 143:159–170.
- Prahlad V, Helfand BT, Landford GM, Vale RD, Goldman RD. 2000. Fast transport of neurofilament protein along microtubules in squid axoplasm. *J Cell Sci* 113:3939–3946.
- Raats JM, Pieper FR, Vree Egberts WT, Verrijp KN, Ramaekers FC, Bloemendal H. 1990. Assembly of amino-terminally deleted desmin in vimentin-free cells. *J Cell Biol* 111:1971–1985.
- Sarria AJ, Nordeen SK, Evans RM. 1990. Regulated expression of vimentin cDNA in cells in the presence and absence of a preexisting vimentin filament network. *J Cell Biol* 111:553–565.
- Shah JV, Flanagan LA, Jammey PA, Leterrier J-F. 2000. Bidirectional translocation of neurofilaments along microtubules mediated in part by dynein/dynactin. *Mol Biol Cell* 11:3495–3508.
- Soellner P, Quinlan RA, Franke WW. 1985. Identification of a distinct soluble subunit of an intermediate filament protein: tetrameric vimentin from living cells. *Proc Natl Acad Sci USA* 82:7929–7933.
- Steinert PM. 1991a. Analysis of the mechanism of assembly of mouse keratin 1/keratin 10 intermediate filaments in vitro suggests that intermediate filaments are built from multiple oligomeric units rather than a unique tetrameric building block. *J Struct Biol* 107:175–188.
- Steinert PM. 1991b. Organization of coiled-coil molecules in native mouse keratin 1/keratin 10 intermediate filaments: evidence for alternating rows of antiparallel in-register and antiparallel staggered molecules. *J Struct Biol* 107:157–174.
- Tint I.S, Hollenbeck PJ, Verkhovsky AB, Surgucheva IG, Bershadsky AD. 1991. Evidence that intermediate filament reorganization is induced by ATP- dependent contraction of the actomyosin cortex in permeabilized fibroblasts. *J Cell Sci* 98:375–384.
- Vikstrom KL, Borisy GG, Goldman RD. 1989. Dynamic aspects of intermediate filament networks in BHK-21 cells. *Proc Natl Acad Sci USA* 86:549–553.
- Windoffer R, Leube RE. 1999. Detection of cytokeratin dynamics by time-lapse fluorescence microscopy in living cells. *J Cell Sci* 112:4521–4534.
- Windoffer R, Beile B, Leibold A, Thomas S, Wilhelm U, Leube RE. 2000. Visualization of gap junction mobility in living cells. *Cell Tissue Res* 299:347–362.
- Yoon M, Moir RD, Prahlad V, Goldman RD. 1998. Motile properties of vimentin intermediate filament networks in living cells. *J Cell Biol* 143:147–157.